arXiv:1403.7586v1 [cond-mat.dis-nn] 29 Mar 2014

Micro-transition cascades to percolation

Wei Chen[1], Malte Schröder[2], Raissa M. D'Souza[3,4], Didier Sornette[5], Jan Nagler[5,2]
[1]*Institute of Computing Technology, Chinese Academy of Sciences, Beijing, China*
[2]*Max Planck Institute for Dynamics and Self-Organization (MPI DS) Göttingen, and Institute for Nonlinear Dynamics, Faculty of Physics, University of Göttingen*
[3]*University of California, Davis, California 95616, USA*
[4]*Santa Fe Institute, 1399 Hyde Park Road, Santa Fe, New Mexico 87501, USA and*
[5]*Department of Management, Technology and Economics (D-MTEC), ETH Zurich, Scheuchzerstrasse 7, CH-8092 Zurich, Switzerland*

We report the discovery of a discrete hierarchy of micro-transitions occurring in models of continuous and discontinuous percolation. The precursory micro-transitions allow us to target almost deterministically the location of the transition point to global connectivity. This extends to the class of intrinsically stochastic processes the possibility to use warning signals anticipating phase transitions in complex systems.

Introduction Percolation is a pervasive concept [1], which has applications in a wide variety of natural, technological and social systems [2–7], ranging from conductivity of composite materials [8, 9] and polymerizations [10] to epidemic spreading [11–13] and information diffusion [14, 15]. Across all percolation systems, once the density of links in the networked system exceeds a critical threshold the system undergoes a sudden usually unanticipated transition to global connectivity.

The prediction of tipping points and warning signals that precede a sudden transition have been a subject of high interest in many disciplines. Generalized models, based on deterministic bifurcation dynamics, have been used to predict phase transitions triggered by small fluctuations [16–20]. Here we report on a fundamental property of percolating systems which, in contrast, are dominated by (non-deterministic) large-scale disorder.

Discrete scale invariance (DSI) arises when the scale invariance of an observable $\mathcal{O}(x) \sim x^\alpha$ obeying $\frac{\mathcal{O}(\lambda x)}{\mathcal{O}(x)} = \lambda^\alpha$, is broken such that the scaling relation does not hold for all λ anymore but only for a countable set $\lambda_1, \lambda_2, ...$ with a fixed λ being the fundamental scaling ratio of the system and $\lambda_n = \lambda^n$ [21, 22]. Here, we unravel both genuine DSI and a generalized form of DSI in percolation, where in the latter the scaling ratio from the exponential is replaced by a scaling law. Analyzing individual events allows us to link these concepts.

Perhaps most importantly, we show that the emergence of global connectivity is announced by microscopic transitions of the largest component, the order parameter, well in advance of the phase transition. We exemplify this for the generalized BFW model of genuinely discontinuous percolation [23, 24], classic continuous percolation [1], and globally competitive percolation [25]. This suggests the universality of our findings.

Discontinuous percolation The generalized Bohman-Frieze-Wormald model (BFW) is tailored to investigate discontinuous percolation transitions resulting from suppressing the growth of the largest component [23], as characteristic of *explosive* percolation. The process is initialized with N isolated nodes and a cap set to $k = 2$ specifying the maximally allowed cluster size (a cluster is a set of linked nodes). Links are sampled one-at-a-time, uniformly at random from the complete network. If a link would lead to the formation of a component of size less than or equal to k it is accepted. Otherwise, the link is rejected provided that the fraction of accepted links is greater than or equal to a function $g(k) = \alpha + (2k)^{-1/2}$, where α is a tunable parameter. Once rejecting a link would lead to the fraction of accepted edges dropping below $g(k)$, then $k \to k + 1$ and the link is reexamined. This continues until either k has increased sufficiently that the link can be accepted, or $g(k)$ becomes sufficiently small that the link can be rejected. (See Supplementary Material [26] for more details.) Tuning the control parameter α allows for controlling the type and position of the phase transition, as well as the number of giant components that abruptly emerge [23, 32]. Fig. 1 shows the typical evolution of the relative size of the largest component C_1/N as a function of the link density p (*i.e.*, number of links per node) for $\alpha = 0.1, 0.3, 0.6$.

The exact size of the largest component for a given link density may depend on the realization. However, in traditional percolation at the thermodynamic limit the order parameter, C_1/N, is believed to be globally continuous and thus not fluctuating—except at the phase transition points [1, 34–36]. In contrast, we next demonstrate that the BFW model exhibits peaks in the relative variance $\mathcal{R}_v$, well *before* the phase transition, which importantly do not disappear in the thermodynamic limit, and moreover, announce the phase transition. The relative variance of an order parameter $\mathcal{O}$, such as the total magnetization $\mathcal{O} = \mathcal{M}$, or the relative size of the largest component $\mathcal{O} = C_1/N$, is defined as

$$\mathcal{R}_v = \frac{\langle \mathcal{O} - \langle \mathcal{O} \rangle \rangle^2}{\langle \mathcal{O} \rangle^2} \tag{1}$$

where $\langle\rangle$ denotes ensemble averaging.

Micro-transition cascades to percolation Fig. 2(a) shows sharp peaks in $\mathcal{R}_v$ well in advance of p_c for the

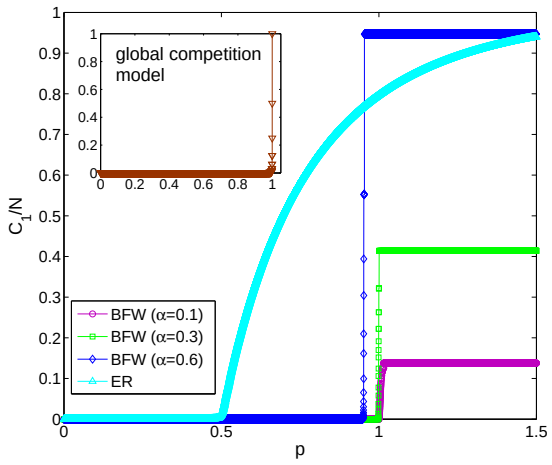

Figure 1: (Color online) **Discontinuous BFW percolation.** A typical realization of the relative size of the largest component C_1/N as a function of link density p for BFW with $\alpha = 0.1, 0.3, 0.6$, and for the continuous ER model. Inset: Discontinuous global competition model. System size $N = 10^6$.

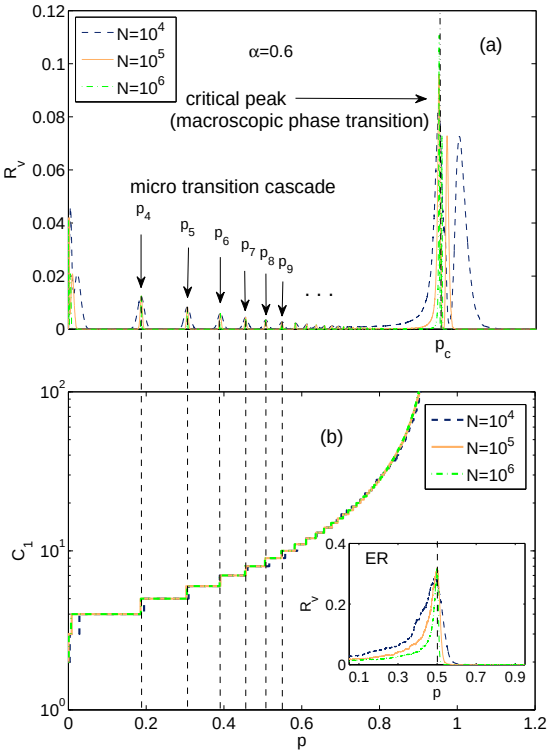

Figure 2: (Color online) **Micro-transition cascade to percolation in the BFW model.** (a) Relative variance R_v versus link density p showing sharp micro-transitions before p_c. Peaks after p_c result from unstable giant components, discussed elsewhere [33]. (b) The typical evolution (and collapse) of C_1 versus p, showing jumps when $C_1 \to C_1+1$. Inset of (b): $\mathcal{R}_v$ versus p for continuous ER percolation, shown for three different system sizes. This reveals a *spectrum* of micro-resonances before $p_c = 1/2$, that, in contrast to the BFW model, disappears as $N \to \infty$. All data shown is the average over 1000 realizations.

BFW model with $\alpha = 0.6$ (figures for $\alpha = 0.1$, 0.3 are in the SI). This is unexpected as suggested from comparing Fig. 2(a), with the $\mathcal{R}_v$ plot for the Erdős-Rényi (ER) model [1] shown in the inset in Fig. 2 (b). In BFW we observe not only the standard transition to global connectivity, which is a *micro-macro-transition*, $C_1 : o(N) \to O(N)$ at $p = p_c$, but as well *micro-micro-transitions*, $C_1 \to C_1 + 1$ causing sharp jumps well before the emergence of global connectivity, Fig. 2(b). Importantly, for increasing system size, the peaks become sharper, their positions converge to a well defined set, and peak heights are independent of system size, see Fig. 2 and Supplementary Figs. S1-S5 [26].

We calculate the height of the $\mathcal{R}_v$ peaks, for jumps $C_1 \to C_1 + 1$, where the i-th jump corresponds to C_1 increasing from $i \to i + 1$ at link density p_i. (The jump $1 \to 2$ occurs always when the first link is added, thus no peak of R_v is observed then.) We estimate the maximum of R_v for the i-th jump by assuming that for a fraction q_i of the realizations $C_1 \to C_1 + 1$, while C_1 for a fraction $1 - q_i$ of the realizations has not increased. Hence, from Eq. (1) we obtain

$$\mathcal{R}_v(p_i) = \frac{q_i(1-q_i)}{(i+q_i)^2} \text{ with } q_i = \frac{i}{2i+1}, \qquad (2)$$

where the q_i's satisfy $\frac{\partial \mathcal{R}_v}{\partial q_i} = 0$. From Eq. 2, we find $q_4 = 4/9$ $q_5 = 5/11$, and $q_6 = 6/13$, and that $\mathcal{R}_v(p_4) \approx 0.0125, \mathcal{R}_v(p_5) \approx 0.0083, \mathcal{R}_v(p_6) \approx 0.0060$ for the $o(N)$-transitions $4 \to 5, 5 \to 6$, and $6 \to 7$, respectively. These predictions are well supported by numerics, see [26].

Analyzing additional peaks as shown in Fig. 3(a) suggests a scaling law of the relative peak positions

$$\frac{p_{i+1} - p_i}{p_i} \approx \log\left(\frac{p_{i+1}}{p_i}\right) = Ai^{-b}, \; i \gg 1 \qquad (3)$$

with b close to 2, slightly depending on α, for some $A > 0$.

We infer p_∞ from Eq. 3 (See [26] for details) and find that $p_\infty = p_c = 0.940, 0.998, 0.999$ for $\alpha = 0.6, 0.3, 0.1$ respectively, which agree exactly with the values of p_c obtained from direct simulation of the BFW model. (See [26] for p_∞ values obtained for additional α values.) In fact, the inset of Fig. 3(a) shows that $p_c - p_i < 0.01$ when $i > 600$ for $\alpha = 0.1, 0.3, 0.6$. Thus we find here that the positions of the micro-transitions announce the phase transition.

Discrete scale invariance in percolation Next we show that a percolation model with global competition for link-addition exhibits a discrete scale invariance that underlies the observed cascade to percolation.

Start with N isolated nodes. At each step connect the two smallest clusters in the system (if there are multiple

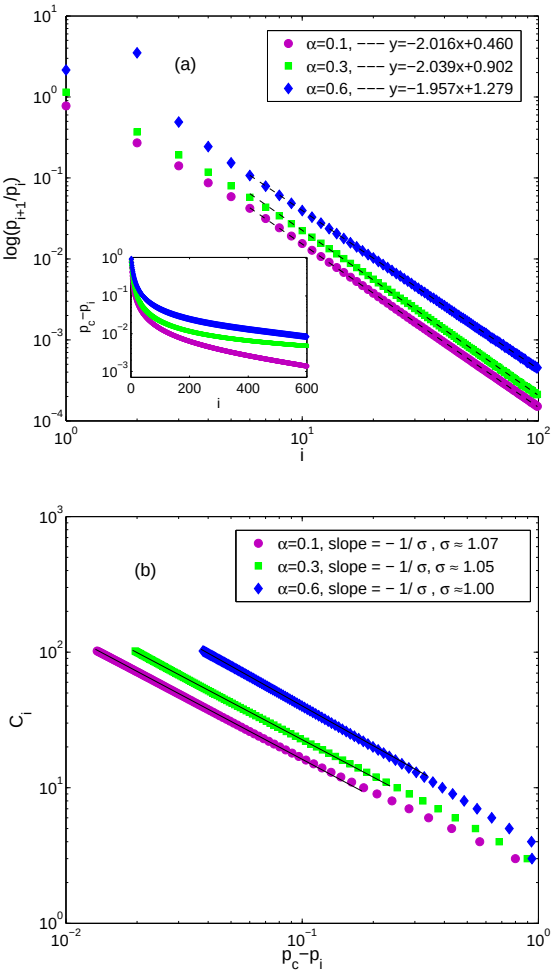

Figure 3: (Color online) **Scaling Laws and Convergence to p_c for the BFW model.** (a) The position p_i of the micro-transitions are well fitted by Eq. 3 for $\alpha = 0.1, 0.3, 0.6$. Note that we display a log-log plot suggesting $\log \frac{p_{i+1}}{p_i} = Ai^{-b}$. Inset of (a): Evidence for $p_i \to p_c$ for $\alpha = 0.1, 0.3, 0.6$ and $N = 10^7$. (b) Exponent σ defined in Eq. (8) for $\alpha = 0.1, 0.3, 0.6$ and $N = 10^7$.

choices, throw a fair dice to choose among the equivalent cluster pairs) [25, 37]. In this model all possible links compete for addition. Thus it is the limiting case $m \to \infty$ of the original explosive percolation models from Ref. [38], where at each step a fixed number of m links compete for addition [25, 37]. The global competition suppresses transitions different from *doubling* transitions $C_1 \to 2C_1$ resulting in $p_c = 1$. For $N \gg 1$ fixed, these occur at $p_n = \frac{2^n-1}{2^n}$, n integer [25], and hence

$$p_n = p_c - 2^{-n},\ n \geq 0 \tag{4}$$

As a result, the doubling transitions announce the percolation transition as $p_n \to p_c$ for $n \to \infty$. This is a signature of discrete scale invariance (DSI) [21, 39] as we

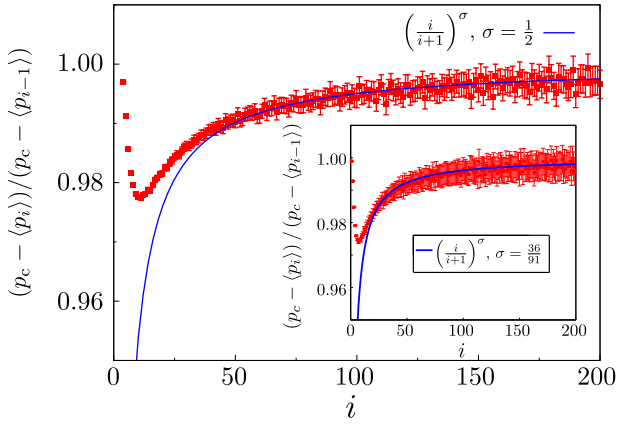
$\left(\frac{i}{i+1}\right)^{\sigma}$, $\sigma = \frac{1}{2}$
$(p_c - \langle p_i \rangle)/(p_c - \langle p_{i-1} \rangle)$
i
$\left(\frac{i}{i+1}\right)^{\sigma}$, $\sigma = \frac{36}{91}$

Figure 4: (Color online) **Scaling relations for continuous percolation.** Numerical evidence for the prediction $\frac{p_c - p_i}{p_c - p_{i-1}} \sim (\frac{i}{i+1})^{\sigma}$ from Eq. (8), for ER ($\sigma = 1/2$, $N = 2^{25}$, 30000 realizations) and 2D lattice ($\sigma = 36/91$, $N = 1024 \times 1024$, 30000 realizations).

can rewrite Eq. (4) to

$$\frac{p_c - p_{n+1}}{p_c - p_n} = 1/\lambda,\ C_1(p_{n+1}) = \lambda C_1(p_n) \tag{5}$$

with the discrete scaling factor $\lambda = 2$.

The DSI can be broken when the system stochastically deviates from the strict size doubling rule, as generically given in percolation and other disordered systems [22]. We thus consider jumps from any size $C_1 \leq i$ to precisely $C_1 = i + 1$. The index transformation $i = 2^{n+1} - 1$ formally breaks the genuine DSI and suggests, using Eq.(4), the transition positions $p_i = 1 - 2/(i + 1)$.

The relative positions of the transitions then read

$$\frac{p_{i+1} - p_i}{p_i} \sim i^{-b}, \text{for } i \gg 1, \tag{6}$$

with $b = 2$, which agrees well with the scaling law Eq. (3). It is easy to see that any transformation of type $n \to \alpha \log(\beta i + \gamma)$, with constants $\alpha, \beta > 0$ and any γ gives the same qualitative result.

Relation to cut-off critical exponent Next we demonstrate that micro-transitions also announce the phase transition well in advance for continuous percolation. In continuous percolation as $p \to p_c$, from below ($p < p_c$), the emergence of the giant cluster is characterized by

$$C_1 \sim (p_c - p)^{-\frac{1}{\sigma}} \tag{7}$$

where σ is the cut-off critical exponent that, given strong disorder, is related to the correlation exponent ν and the fractal dimension d_f via $\sigma = \frac{1}{\nu d_f}$ [1, 27].

We estimate the positions of the micro-transitions at p_i from (7) for $C_1 = i + 1$ and $p = p_i$. Solving for p_i gives

$$p_i = p_c - A(i + 1)^{-\sigma} \tag{8}$$

with some prefactor $A > 0$. From Eq. (8) we find

$$\frac{p_{i+1} - p_i}{p_i} \approx \frac{A[(i+1)^{-\sigma} - (i+2)^{-\sigma}]}{p_c} \sim i^{-(1+\sigma)} \text{ for } i \gg 1. \tag{9}$$

This equation predicts for *any* phase transition characterized by the exponent σ a cascade defined by Eqs. (6) and (9) with exponent $b = 1 + \sigma$.

Above the percolation upper critical dimension, and thus for ER percolation, the set of critical percolation exponents are known, $\sigma = \nu = 1/2$, $d_f = 4$ [1]. For ER, Eq. (8) is well supported by numerics, see Fig. 4. Further, numerics for 2D site-percolation, where $\sigma = \frac{1}{\nu d_f} = \frac{1}{4/3\ 91/48} \approx 0.396$ is known from theory [1], well supports our prediction (see inset in Fig. 4).

Specifically, we define p_i as the position of the micro-transition of the type $C_1 : x \to i + 1$ $(x \leq i)$. Since for a given realization a jump of this type and thus p_i may not exist, to obtain $\langle p_i \rangle$ in Fig. 4, we average for each i over all realizations where $C_1 : x \to i+1$ $(x \leq i)$ do occur and p_i is well defined,

$$\langle p_i \rangle := \langle \arg_{\exists (i, x \leq i)} \{C_1(p) : x \to i + 1\} \rangle \tag{10}$$

In contrast, for fixed N, most pronounced close to the origin at $p = 0$, micro-transitions localize but ensemble averaging 'blurs out' peaks in $\mathcal{R}_v$ for larger values of p (see Figs. S7 and S8 [26]).

For the BFW model we find the exponent σ, slightly depending on α, close to unity, see Fig. 3(b). This result is in agreement with Eq. (6), predicting $b \approx 2$, and with the numerics shown in Fig. 3(a).

For the globally competitive percolation model we calculate for $p < p_c$ [25, 40]

$$C_1 = \frac{N}{N - L} = \frac{1}{1 - p} = (p_c - p)^{-\frac{1}{\sigma}},\ p = L/N, \tag{11}$$

with $\sigma = 1$, which is an exact result.

Further, from Eq. (7) we calculate the relative positions for transitions of type $C_1 \to nC_1$, for $n > 1$ fixed,

$$\frac{p_c - p_{ni}}{p_c - p_i} \to n^{-\sigma} = n^{1-b} =: 1/\lambda^{(n)},\ \text{for } i \to \infty. \tag{12}$$

Eq. (12) describes a family of micro-transition scaling relations parametrized by n.

We can also turn Eq. (12) around for predicting p_c. For the ER model we find for $n = 2$, $\lambda^{(2)} = 2^{\sigma} = \sqrt{2}$ and

$$p_c = \lim_{i \to \infty} \frac{\lambda^{(2)} p_{2i} - p_i}{\lambda^{(2)} - 1}. \tag{13}$$

Numerical evaluation of (13) suggest $p_c = 0.499585$ for $i = 128$, which is close to the exact value $p_c = 0.5$ [1].

Conclusion We have established the appearance of well defined peaks in the subcritical regime for standard processes of continuous and discontinuous percolation. The cause of those resonances in the relative fluctuation function are micro-transitions of type $o(N) \to o(N)$ that generically announce the percolation phase transition well in advance of p_c. Therefore, genuine peaks in the relative variance do not necessarily indicate a phase transition point, as it is commonly exploited for characterization of the phase transition point in classical and quantum critical systems [27]. We have discovered an overlooked phenomenon, micro-transition cascades in percolation, which as shown here can result from a (generalized) discrete scale invariance of the order parameter at and before criticality.

Globally competitive percolation displays genuine discrete scale invariance where the positions of the micro-transitions are characterized by powers of the single fundamental scaling factor $\lambda = 2$. This results from a single route of doubling transitions of the order parameter, for large finite systems.

In contrast, we have demonstrated that systems with strong disorder display multiple micro-transition cascades to percolation that are not characterized by a single scaling factor but by a set of scaling relations, exemplified for percolation. The simplest subset of these scaling relations describe transitions $C_1 \to nC_1$, $n \geq 2$ integer, which occur at localized positions, for large finite systems. We call this phenomenon generalized discrete scale invariance in percolation.

We have established a novel type of finite size scaling laws which crucially characterize percolation. As our arguments are independent of the percolation process and the system size, for any $N < \infty$ there necessarily exist cascades to percolation imprinted both in the order parameter and its relative variance. Exemplified for a well-studied discontinuous percolation process, we have shown that these cascades can even survive the thermodynamic limit.

Continuous percolation exhibits a continuous power law divergence at p_c that does not show any localized peaks in the relative variance in the thermodynamic limit. In contrast, for fixed N, micro-transitions do localize albeit ensemble averaging blurs out peaks in $\mathcal{R}_v$. Ensemble averaging in accords with Eq. 10, however, robustly unravels the discrete hierarchy and thus overcomes the effect of blurring.

We find DSI and its (exponential or power law) scaling laws from a non-trivial exponentiation ($C_1 \to \lambda C_1$ at $p_i \to p_{i+1}$) of a discrete translational invariance resulting from the discreteness of the network, or lattice [21].

Hence, a percolation phase transition can be anticipated by inferring information from ensemble averaged microscopic state changes of the order parameter well in advance of the transition point. Thus we are able to extend the possibility of early warning signals to classes of

stochastic dynamics. Future work must establish if these findings will open new avenues for the prediction of phase transitions unrelated to percolation.

This work was funded by the 973 National Basic Research Program of China under grant numbers 2013CB329602 and 2012CB316303, the National Natural Science Foundation of China under grant numbers 61232010 and 11305219, National High Technology Research and Development Program of China under grant number 2014AA015103, the Defense Threat Reduction Agency HDTRA1-10-1-0088, and the Army Research Office awards W911NF-09-2-0053 and W911NF-13-1-0340.

[1] D. Stauffer and A. Aharony. *Introduction to Percolation Theory* (Taylor & Francis, London, 1994).
[2] B. Drossel and F. Schwabl, *Phys. Rev. Lett.* **69**, 1629-1632 (1992).
[3] S. V. Buldyrev, R. Parshani, G. Paul, H. E. Stanley, and S. Havlin. *Nature* **464**, 1025-1028 (2010).
[4] M. E. J. Newman, D. J. Watts, and S . H. Strogatz. *Proc. Natl. Acad. Sci.* **99**, 2566-2572 (2002).
[5] D. S. Callaway, M. E. J. Newman, S. H. Strogatz, and D. J. Watts *Phys. Rev. Lett.* **85**, 5468-5471 (2000).
[6] G. Gaillard-Groleas, M. Lagier, and D.Sornette, *Phys. Rev. Lett.* **64**, 1577-1580 (1990).
[7] A. A. Saberi, *Phys. Rev. Lett.* **110**, 178501 (2013).
[8] J. S. Andrade, S. V. Buldyrev, N. V. Dokholyan, S. Havlin, P. R. King, Y. K. Lee, G. Paul, and H. E. Stanley, *Phys. Rev. E* **62**, 8270 (2000).
[9] M. Sahimi. *Applications of Percolation Theory* (Taylor & Francis, London, 1994).
[10] R. M. Ziff, E. M. Hendriks, and M. H. Ernst, *Phys. Rev. Lett.* **49**, 593 (1982).
[11] C. Moore and M. E. J. Newman, *Phys. Rev. E* **61**, 5678 (2000).
[12] R. Pastor-Satorras and A. Vespignani, *Phys. Rev. Lett.* **86**, 3200 (2001).
[13] R. M. Anderson and R. M. May. *Infectious Diseases of Humans*. (Oxford University Press, New York, 1991).
[14] D. Strang and S. Soule, *Annual Review of Sociology* **24**, 265290 (1998).
[15] P. F. Lazarsfeld, B. Berelson, and H. Gaudet, *The People's Choice*. (Columbia University Press, New York, 1944).
[16] M. Scheffer, et al. Nature **461**, 53 (2009).
[17] C. Boettiger, A. Hastings, *Nature* **493**, 157-158 (2013).
[18] C. Boettiger, N. Ross, A. Hastings, *Theor. Ecol.* **6**, 255-264 (2013).
[19] L. Dai, D. Vorselen, K. Korolev, and J. Gore, *Science* **336**, 1175-1177 (2012).
[20] L. Dai, K. S. Korolev, and J. Gore, *Nature* **496**, 355-358 (2013).
[21] D. Sornette, Physics Reports **297**(5), 239-270 (1998).
[22] D. Sornette, *Critical Phenomena in Natural Sciences, Chaos, Fractals, Self-organization and Disorder: Concepts and Tools* (Springer Series in Synergetics, Heidelberg, 2004).
[23] W. Chen and R. M. D'Souza, Phys. Rev. Lett. **106**, 115701 (2011).
[24] K. J. Schrenk, A. Felder, S. Deflorin, N. A. M. Araújo, R. M. D'Souza, and H. J. Herrmann, Phys. Rev. E **85**, 031103 (2012).
[25] J. Nagler, A. Levina, and M . Timme, *Nat. Phys.* **7,** 265-270 (2011).
[26] See Supplemental Material [url], which includes Refs. [27-33].
[27] H. E. Stanley, *Introduction to Phase Transitions and Critical Phenomena* (Oxford University Press, Oxford and New York, 1971)
[28] H. Saleur and D. Sornette, J. Phys. I France **6**(3), 327-355 (1996).
[29] P. Erdős and A. Rényi. *Publ. Math. Inst. Hungar. Acad. Sci.* **5** (17) (1960).
[30] T. Bohman, A. Frieze, and N. C. Wormald. *Random Structures & Algorithms* 25(4):432-449, (2004).
[31] W. Chen, J. Nagler, X. Cheng, X. Jin, H. Shen, Z. Zheng and R. M. D'Souza, *Phys. Rev. E* 87, 052130 (2013).
[32] W. Chen, Z. Zheng, and R. M. D'Souza, Europhys. Lett. **100**(6), 66006 (2012).
[33] W. Chen, X. Cheng, Z. Zheng, N. N. Chung, R. M. D'Souza, J. Nagler, Phys. Rev. E **88**, 042152 (2013).
[34] O. Riordan, and L. Warnke, *Science* **333,** 322-324 (2011).
[35] O. Riordan, and L. Warnke, *Phys. Rev. E.* **86,** 011129 (2012).
[36] A. Aharony, and A. B. Harris, *Phys. Rev. Lett.* **77,** 3700-3703 (1996).
[37] E. J. Friedman, and A. S. Landsberg, *Phys. Rev. Lett.* **103**, 255701 (2009).
[38] D. Achlioptas, R. M. D'Souza, and J. Spencer, *Science* **323**, 1453-1455 (2009).
[39] K. Ide and D. Sornette, Physica A **307** (1-2), 63-106 (2002).
[40] M. Schröder, S. H. Ebrahimnazhad Rahbari, and J. Nagler, *Nature Commun.* **4**:2222, (2013).

arXiv:1403.7586v1 [cond-mat.dis-nn] 29 Mar 2014

Supplementary Information:

Micro-transition cascades to percolation

Wei Chen, Malte Schröder, Raissa M. D'Souza, Didier Sornette, Jan Nagler

Here we provide supplementary information to the main manuscript.

S.1 Additional notes to the notion of discrete scale invariance (DSI)

DSI is the partial breaking of continuous scale invariance [1, 2] in the sense that the scale invariance only holds for magnification factors (or scaling factor) that are integer powers of a fundamental scaling ratio. For instance, the standard Cantor set defined as a segment divided in 3 parts in which the central segment is deleted, and the operation is repeated ad infinitum, exhibits the property of DSI with a fundamental scaling ratio of 3 [3].

The key idea here is that it is a kind of exponentiation of the discrete increase $C_1 \to C_1 + 1$ (or $C_1 \to C_1 + n$) that leads to DSI and its generalization ($e^{C_1} \to e^{C1} * e^{a*1}$, where a depends on the physical or geometrical problem). Hence the scaling ratio λ comes from the transformation by a kind of exponentiation of the discrete translational invariance of a discrete growing process. In particular, our micro-transitions can be seen as macro-evidence of the existence of an underlying discrete lattice or process combined with the cooperation / connectivity associated with the percolation rules.

The simplest case of the exponentiation of DSI occurs in the global competition percolation model and is described by $C_1 \to \lambda C_1$ such that $C_1^{(n)} = \exp(\log(\lambda)n)C_1(n_0)$, $\lambda = \text{const.} = 2$, $n = 1, 2, ...$ (see Eq. (5) in the main text). Thus we find discrete jumps of an extremal stochastic variable (here the order parameter C_1) whose micro-transition positions p_n (or p_i) are described by scaling laws characterizing the translational invariance of the system, or analogously, the waiting times between extremal growth events (in C_1). In general, this genuine DSI is broken such that the exponential of $\log(\lambda)n$ is replaced by a more complex expression such as power law scaling relations (Eqs. (5) and (11) in the main text).

The order parameter of continuous percolation becomes perfectly smooth in the limit $N \to \infty$, exhibiting a typical power law divergence of the order parameter at p_c. DSI relates to finite size ($N < \infty$) scaling laws in p_i which robustly announce p_c. As being evident from our study the announcement begins well in advance of p_c for both the continuous and discontinuous models which is thus unrelated to the standard (dis)continuous divergence close to p_c. In order to be able to make a general argument we focus on the characterizations of the p_i close to p_c where we find clean scaling laws which then connect to the critical cut-off exponent σ.

To summarize, we find DSI and its (exponential or power law) scaling laws from a non-trivial exponentiation of a discrete translational invariance of the positions of micro-transitions of an extremal stochastic variable (the order parameter C_1).

S.2 Connection to Lattice Animals

We have demonstrated that micro-transitions occur in four different percolation models, which shows that they are not an artifact of a specific construction method. Instead, they actually result from the discrete nature of the lattice or network, in a kind of exponentiation of the translational invariance of integer increase to (discrete) scale invariance across scales. This is in agreement with the finding that lattice animals in percolation do show discrete scale invariance [4]. The novelty here is that the information on p_c is already contained in the discrete scaling of the small clusters.

S.3 The Bohman-Frieze-Wormald algorithm

Stating the BFW model explicitly, it begins with a collection of N isolated nodes and proceeds in phases starting with $k = 2$, which is the maximally allowed cluster size. Edges are sampled one at a time, uniformly at random from the complete graph induced on the N nodes. Using the notation in [6], let u denote the total number of edges sampled, A the set of accepted edges (initially $A = \emptyset$), and $t = |A|$ the number of accepted edges. At each step u, the selected edge e_u is examined via the following algorithm (the BFW algorithm):

```
Set l = maximum size component in A ∪ {e_u}
   if (l ≤ k) {
      A ← A ∪ {e_u}
      u ← u + 1 }
   else if (t/u < g(k)) { k ← k + 1 }
   else { u ← u + 1 }
```

Walking through the loop, if adding e_u leads to a component of size $l \leq k$, the edge is added and step u completes and we move onto step $u + 1$. Otherwise, check if $t/u < g(k)$. If not, then $t/u \geq g(k)$ and e_u is ignored (*i.e.* rejected) and we move onto step $u+1$. If instead it is the case that $t/u < g(k)$ then we augment k and walk through from the "if" loop from the start again. In other words, while $t/u < g(k)$, k is augmented by one repeatedly until either k becomes large enough that edge e_u is accepted or $g(k)$ decreases sufficiently that edge e_u can be rejected at which point step u finally ends. Note $g(k) = 1$ requires that all edges be accepted, equivalent to Erdős-Rényi [5]. Also we use the "min" function, $g(k) = \min\left(1, 1/2 + (2k)^{-\beta}\right)$, to ensure $g(k) \leq 1$ for all choices of β, since the fraction of nodes accepted cannot exceed unity.

T. Bohman, A. Frieze, and N. C. Wormald established rigorous results whereby setting $g(200) = 1/2$, all components are no larger than $k = 200$ nodes (*i.e.*, no giant component exists) when $m = 0.96689N$ edges out of $2m$ sequentially sampled random edges have been added to graph [6]. They further establish that a giant component must exist by the time $m = c^*N$ out of $2m$ sampled edges have been added, with $c^* \in [0.9792, 0.9793]$. Yet, they did not analyze the nature of the percolation transition.

In [7] it was shown that the original BFW model leads to the simultaneous emergence of two giant components (each with fractional size $C > 0.4$), and the stability of the multiple giants was analyzed. (Essentially, once in the supercritical regime, there are always sufficient edges internal to components sampled that whenever an edge connecting two giant components is sampled it can be rejected.) It was also shown in [7] that by using the function $g(k) = \alpha + (2k)^{-1/2}$, then the parameter α tunes the number of stable giant components that emerge simultaneously. For suitable choice of α, a second continuous transition appears in the supercritical regime, leading to the emergence of a second giant component after the percolation threshold [8]. The underlying mechanism for the discontinuous transition occurring in the BFW model is the domination of the overtaking mechanism in the growth of the largest component [9].

S.4 Micro-transition cascade to percolation

In the main manuscript, it was shown that sharp peaks result from micro-micro-transitions $C_1 \to C_1 + 1$ before the emergence of global connectivity for BFW model with $\alpha = 0.6$. Fig. S1 and Fig. S2 show sharp

peaks well in advance of p_c for BFW model with $\alpha = 0.3$ and 0.1 respectively, which were also caused by the micro-micro-transitions $C_1 \to C_1 + 1$. Furthermore, the position of peaks converge to a well-defined set and the peaks do not disappear as the system size increases for BFW model with $\alpha = 0.6, 0.3, 0.1$, as Fig. S3 , Fig. S4 and Fig. S5 show respectively. Fig. S1 and Fig. S2 show that for $\alpha = 0.3$ and 0.1 multiple peaks appear for finite system, however, these multiple peaks shrink into one peak as system size $N \to \infty$. However, for some values of α, multiple peaks survive as $N \to \infty$ which results from unstable giant components, discussed elsewhere [10].

From the main manuscript, for the BFW model, the p_i for the jump $C_1 : i \to i + 1$ satisfy a recurrence relation of the form

$$p_{i+1} = \exp(Ai^{-b})p_i \tag{S1}$$

with b close to 2, and $A > 0$, see fig. 5 (a) in the main manuscript. Rewriting the recurrence relation Eqn. (S1) as

$$p_i = p_{i_0} \exp\left(A((i-1)^{-b} + (i-2)^{-b} + ... + i_0^{-b})\right) \tag{S2}$$

where $i > i_0$. We set $i_0 = 50$ in Eqn. (S2) since the recurrence relation between p_{i+1} and p_i holds for not too small i, let $i \to \infty$, we numerically obtain $p_\infty = 0.999(1), 0.998(1)$ for $\alpha = 0.1, 0.3$ respectively. On the other hand, we estimate percolation threshold p_c by measuring the asymptotic location of the largest jump in the order parameter induced by adding a single edge. We numerically obtain that $p_c = 0.999(1), 0.998(1)$ for $\alpha = 0.1, 0.3$ respectively, which are equal to p_∞ within error bars. We further compare p_∞ with p_c for more values of $\alpha > 0.6$ where the percolation threshold p_c is significantly smaller than 1. We numerically obtain that for $\alpha = 0.8$, $b \approx 1.985, A \approx 7.628, p_{i_0} \approx 0.72(1), p_\infty = 0.85(1), p_c = 0.86(1)$, for $\alpha = 0.75, b \approx 1.952, A \approx 5.418, p_{i_0} \approx 0.76(1), p_\infty = 0.88(1), p_c = 0.89(1)$, and for $\alpha = 0.7, b \approx 1.948, A \approx 4.543, p_{i_0} \approx 0.80(1), p_\infty = 0.90(1), p_c = 0.91(1)$ (See Fig. S6 in detail). Thus we have p_∞ and p_c are almost equal within error bars for various α.

S.5 Derivation of the p_i for the (generalized) BFW model

To obtain the values of p_i for a more generalized model, we assume that the form of $g(k)$ in the BFW algorithm is $g(k) = \alpha + (\gamma k)^{-\beta}$ $(\alpha > 0, \beta > 0, \gamma > 0)$. Let the probability of sampling an edge which leads to a component of size not larger than k at stage k be $P(k, t, u)$. Begin with stage $k = 2$ and at the location of the transition $C_1 : 2 \to 3$, about $p_2 * N$ edges have been added to the graph since the number of self-edges and multiple edges are of order $o(N)$ and can be omitted. At stage $k = 2$, the number of added edges satisfy $0 < t \leq p_2 * N$ and the probability of sampling an edge which leads to a component of size no larger than $k = 2$ is (only an edge that connects two isolated nodes can be added to the system)

$$P(2, t, u) = (1 - \frac{2t}{N})^2 = (1 - 2p)^2 \tag{S3}$$

where $p = t/N$. We next analytically obtain p_2 for two cases: (i): $g(2) < 1$; (ii) $g(2) \geq 1$. If $g(2) < 1$, from the BFW algorithm, at $p = t/N = p_2$, an edge e_u that leads to a component of size larger than $k = 2$ is sampled, since the fraction of accepted edges over randomly sampled edges, t/u, satisfies

$$t/u < g(2), \tag{S4}$$

then k increases from 2 to 3 according to BFW algorithm. We can also obtain that

$$t/(u-1) \geq g(2). \tag{S5}$$

The reason of above inequality (S5) is the following. Assume that (S5) does not hold and $t/(u-1) < g(2)$, then the sampled edge e_{u-1} must lead to a component of size no larger than $k = 2$ and it is accepted, resulting in

$$(t-1)/(u-1) < t/(u-1) < g(2) \tag{S6}$$

Because otherwise e_{u-1} leads to a component of size larger than $k = 2$ and it is rejected, since $t/(u-1) < g(2)$ holds according to our assumption, k would increase from 2 to 3 at step $u-1$, which violates our condition that k increase from 2 to 3 at step u. Then we analyze the situation of the edge sampled at step e_{u-2}. If this edge leads to a component of size larger than $k = 2$ it is rejected. Since $t/(u-1) < g(2)$ and $g(2) < 1$, we have $(t-1)/(u-2) < g(2)$, so e_{u-2} would lead to k increase from 2 to 3 at step $u-2$ which is a contradiction. So we have that e_{u-2} leads to a component of size no larger than $k = 2$ and it is accepted, resulting in

$$(t-2)/(u-2) < (t-1)/(u-1) < g(2). \tag{S7}$$

With a similar analysis, we recursively obtain that for all steps $m < u$, e_m leads to a component of size no larger than $k = 2$ and it is accepted, resulting in

$$(t-(u-m))/m < g(2) \tag{S8}$$

Specifically for the step $m = 1$ (the first step), from Eq. S8, we have $t-(u-m) < 1$, which is impossible. Since the system is initialized with isolated nodes and the first sampled edge would always lead to a component of size no larger than $k = 2$ the edge is accepted, which results in $t-(u-m) = 1$ (or $|A| = 1$, A is the set of edges accepted or added to the graph) and $m = 1$ (number of sampled edges). So we obtain a contradiction which is due to our incorrect assumption that $t/(u-1) < g(2)$. Thus Eq. (S5) holds.

Combining Eqs. (S4) and (S5) for $N \to \infty$, we have following equation at $p = t/N = p_2$,

$$\frac{t/N}{u/N} = g(2). \tag{S9}$$

For the case $g(k) \geq 1$, it is much simpler. Since all sampled edges would be accepted by the BFW algorithm, we have

$$\frac{t/N}{u/N} = 1. \tag{S10}$$

Combining

$$\int \mathrm{d}u/N = \int \frac{\mathrm{d}(t/N)}{P(2,t,u)} \tag{S11}$$

with $t/N = p_2$ and Eq. (S3), we have $u/N = \int_0^{p_2} \frac{1}{(1-2p)^2} dp$ as $N \to \infty$. With Eqs. S9 and S10 this results into

$$\min(1, g(2)) * \int_0^{p_2} \frac{1}{(1-2p)^2} dp = p_2. \tag{S12}$$

If $g(2) > 1$ in Eq. (S12), since $\frac{1}{(1-2p)^2} > 1$, we necessarily have $p_2 = 0$. Specifically, we investigate the cases of $\alpha = 0.1, 0.3, 0.6, \beta = 0.5, \gamma = 2$ as studied in our paper. Since $g(2) = 0.6 < 1$ for $\alpha = 0.1$ and $g(2) = 0.8 < 1$ for $\alpha = 0.3$, replace g(2) in Eq. (S12) and we get $p_2 = 0.2$ for $\alpha = 0.1$ and $p_2 = 0.1$ for $\alpha = 0.3$. However, for $\alpha = 0.6$, $g(2) = 1.1 > 1$, we have $p_2 = 0$. These results are consistent with observations from our numerical simulations (see figure S4 and S5 in the SI).

We can also further obtain p_3 in a similar way. Firstly, at $p = t/N = p_3$, an edge e_u that leads to a component of size larger than $k = 3$ is sampled, and using same analysis as above we have

$$t/u < g(3) \leq t/(u-1) \tag{S13}$$

For $N \to \infty$, we have the following equation at $p = t/N = p_3$

$$\frac{t/N}{u/N} = \min(1, g(3)) \tag{S14}$$

replace $t/N = p_3$ and $u/N = \frac{p_2}{\min(1,g(2))} + \int_{p_2}^{p_3} \frac{1}{P(3,t,u)} dp$ in Eq. (S14), we have

$$\frac{p_3}{\frac{p_2}{\min(1,g(2))} + \int_{p_2}^{p_3} \frac{1}{P(3,t,u)} dp} = \min(1, g(3)) \tag{S15}$$

in which, the form of P(3,t,u) is more complicated than $P(2,t,u)$ and we do not show it here. We can further calculate $p_i(i>3)$ recursively with the following relation

$$\frac{p_i}{\frac{p_{i-1}}{\min(1,g(i-1))}+\int_{p_{i-1}}^{p_i}\frac{1}{P(i,t,u)}dp}=\min(1,g(i)). \tag{S16}$$

Since $g(i)$ is strictly decreasing, we easily obtain from Eq. (S16) that $p_i=p_{i-1}=...=p_2=0$ for $g(i)\geq 1$ while $p_i>0$ for $g(i)<1$.

References

[1] H. E. Stanley, *Introduction to Phase Transitions and Critical Phenomena* (Oxford University Press, Oxford and New York, 1971)

[2] D. Sornette, *Critical Phenomena in Natural Sciences, Chaos, Fractals, Self-organization and Disorder: Concepts and Tools* (Springer Series in Synergetics, Heidelberg, 2004).

[3] D. Sornette, Physics Reports **297**(5), 239-270 (1998).

[4] H. Saleur and D. Sornette, J. Phys. I France **6**(3), 327-355 (1996).

[5] P. Erdős and A. Rényi. *Publ. Math. Inst. Hungar. Acad. Sci.* **5** (17) (1960).

[6] T. Bohman, A. Frieze, and N. C. Wormald. *Random Structures & Algorithms* 25(4):432-449, (2004).

[7] W. Chen and R. M. D'Souza. *Phys. Rev. Lett.* 106, 115701 (2011)

[8] W. Chen, J. Nagler, X. Cheng, X. Jin, H. Shen, Z. Zheng and R. M. D'Souza, *Phys. Rev. E* 87, 052130 (2013).

[9] W. Chen, Z. Zheng, and R. M. D'Souza, *Europhys. Lett.* 100, 66006 (2012).

[10] W. Chen, X. Cheng, Z. Zheng, N. N. Chung, R. M. D'Souza, J. Nagler, Phys. Rev. E **88** 042152 (2013).

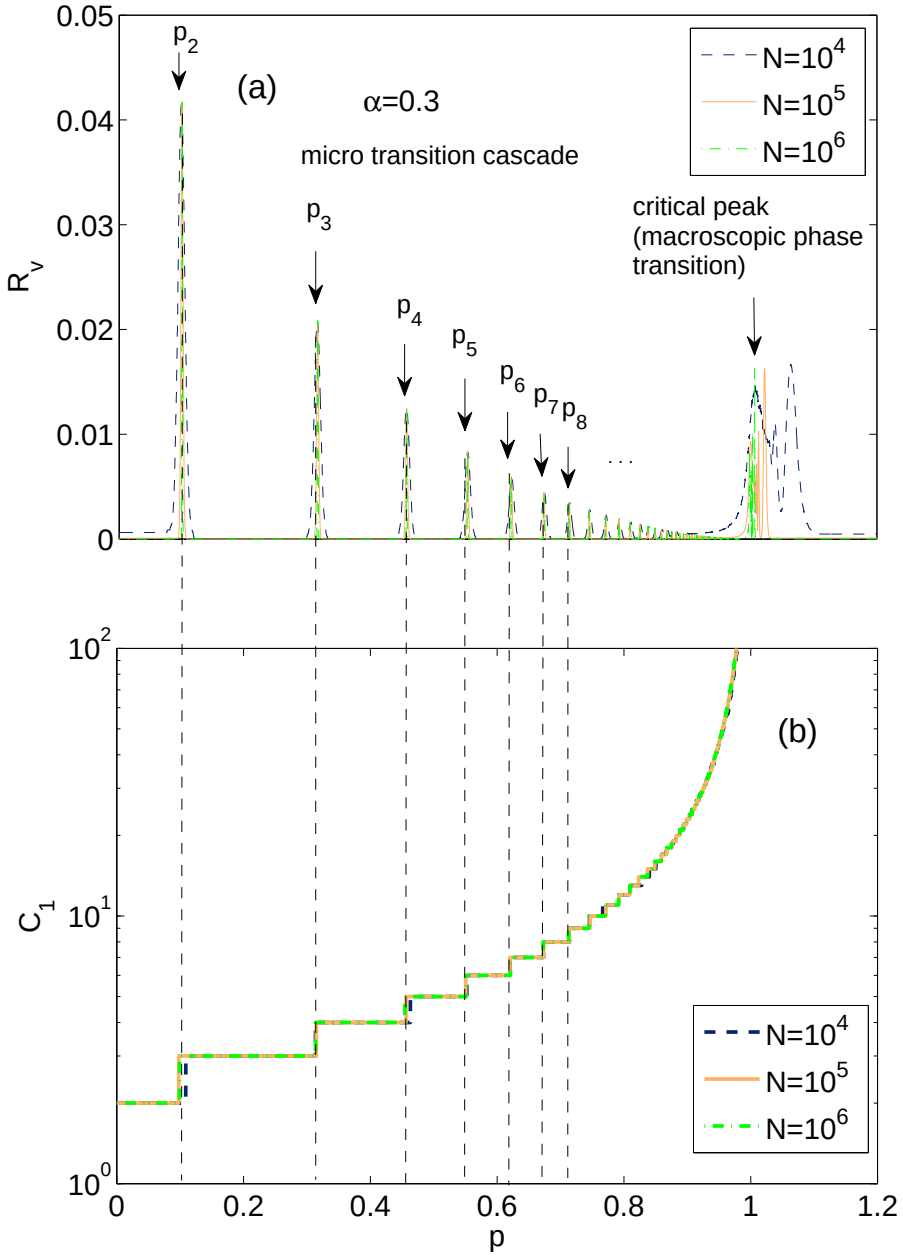

Figure S1: BFW model with $\alpha = 0.3$: (a) relative variance R_v versus edge density p. Infinite sharp micro-transitions before p_c and multiple peaks at p_c. (b) The typical evolution of C_1 versus p, showing the microscopic jumps $C_1 \to C_1 + 1$ occurs at the peaks of R_v before p_c.

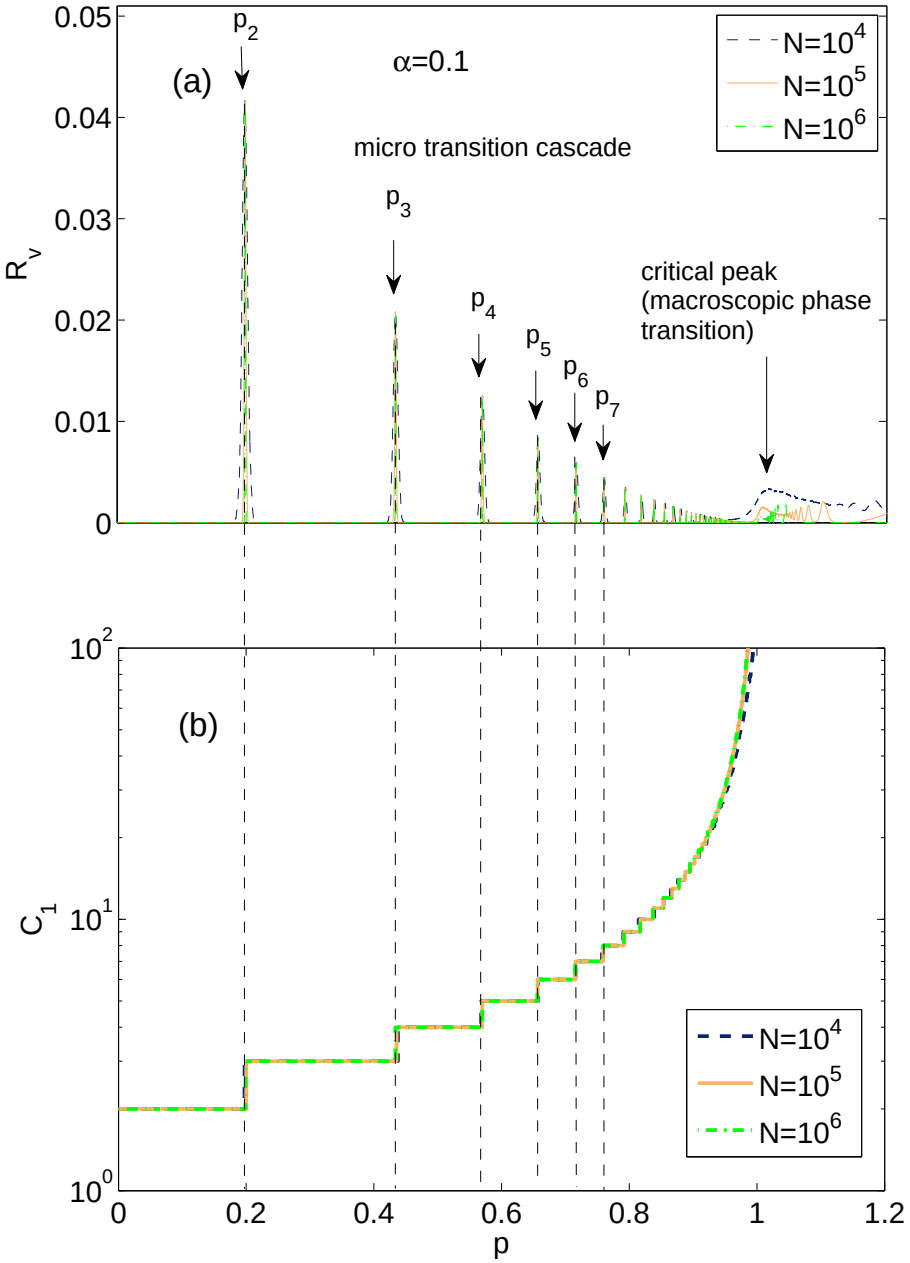

Figure S2: BFW model with $\alpha = 0.1$: (a) relative variance R_v versus edge density p. Infinite sharp micro-transitions before p_c and multiple peaks at p_c. (b) The typical evolution of C_1 versus p, showing the microscopic jumps $C_1 \to C_1 + 1$ occurs at the peaks of R_v before p_c.

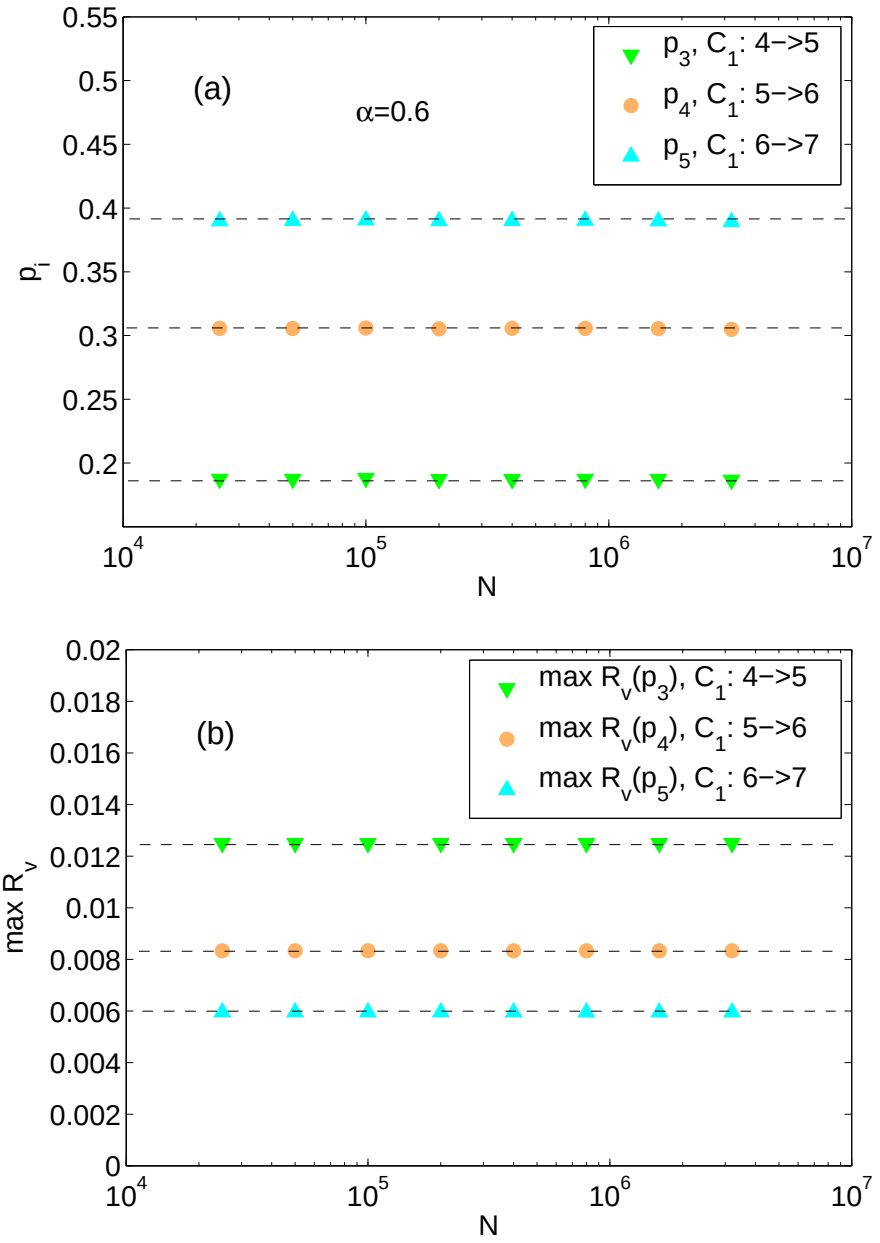

Figure S3: Localization of the peaks for the BFW model with $\alpha = 0.6$: (a) The location of the i-th peaks of $\mathcal{R}_v$, $p_i, i = 3, 4, 5$ is independent of the system size N for BFW model with $\alpha = 0.6$. (b) The heights of the i-th peaks of $\mathcal{R}_v$, $\mathcal{R}_v(p_4), \mathcal{R}_v(p_5), \mathcal{R}_v(p_6)$ are independent of the system size N. $\mathcal{R}_v(p_i)$ with $i > 6$ are also independent of the system size N, which are not shown for space constraints.

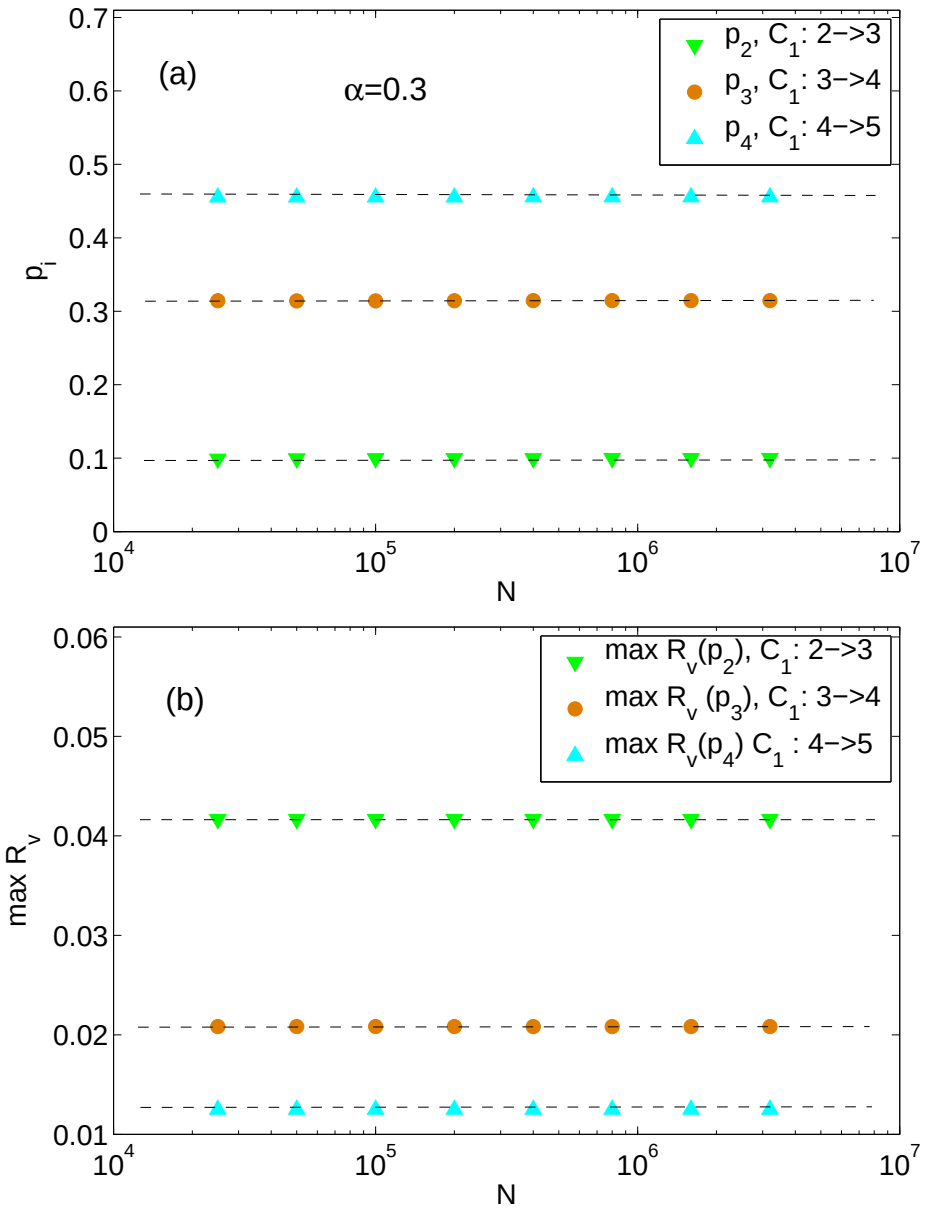

Figure S4: BFW model with $\alpha = 0.3$: (a) the location of the $i-th$ peaks of R_v, $p_i, i = 2, 3, 4$ is independent of the system size N for BFW model with $\alpha = 0.3$. (b) the heights of the $i-th$ peaks of R_v, $R_v(p_2), R_v(p_3), R_v(p_4)$ are independent of system size N. $R_v(p_i)$ with $i > 4$ are also independent of the system size N, which are not shown for space constraints.

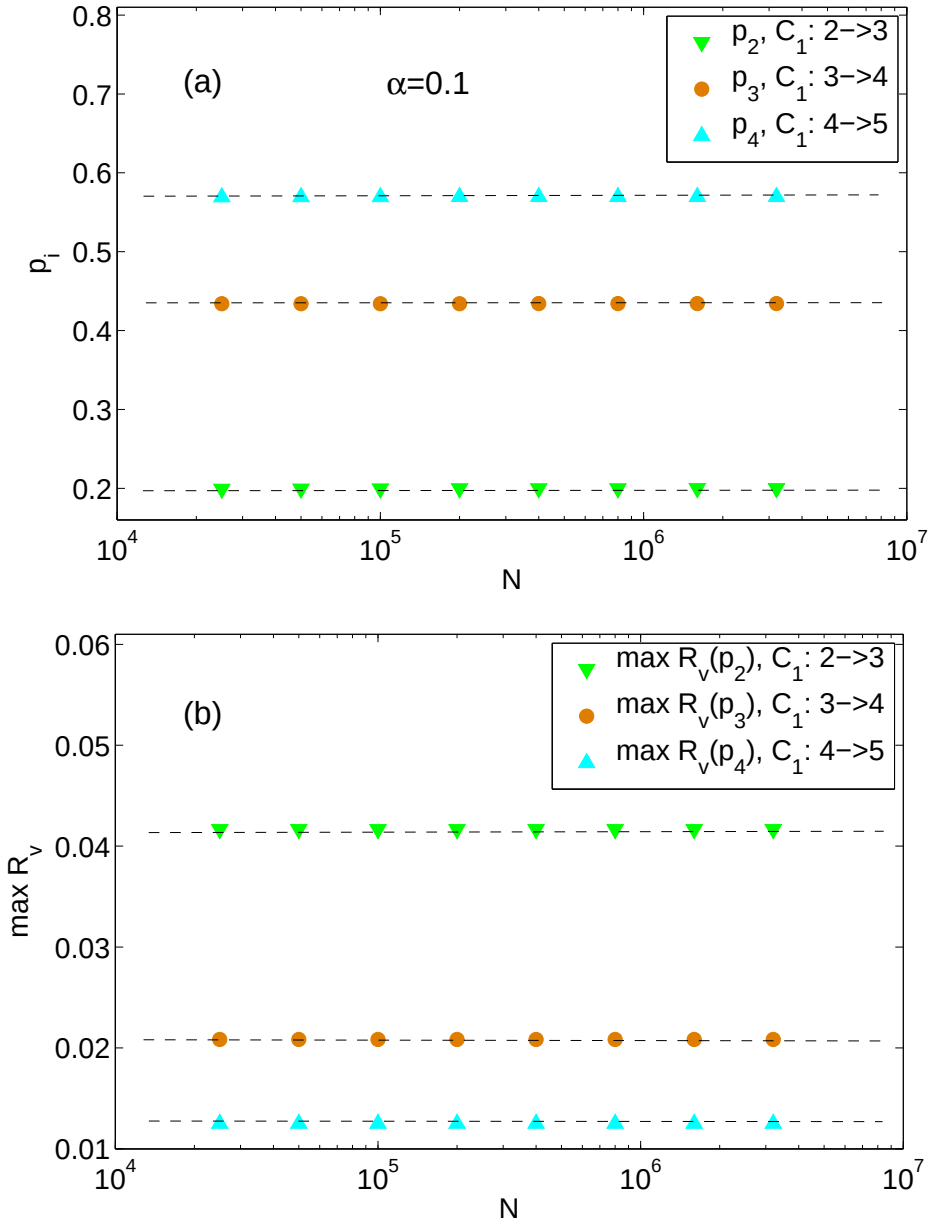

Figure S5: BFW model with $\alpha = 0.1$: (a) the location of the $i-th$ peaks of R_v, $p_i, i = 2, 3, 4$ is independent of the system size N for BFW model with $\alpha = 0.1$. (b) the heights of the $i-th$ peaks of R_v, $R_v(p_2), R_v(p_3), R_v(p_4)$ are independent of system size N. $R_v(p_i)$ with $i > 4$ are also independent of the system size N, which are not shown for space constraints.

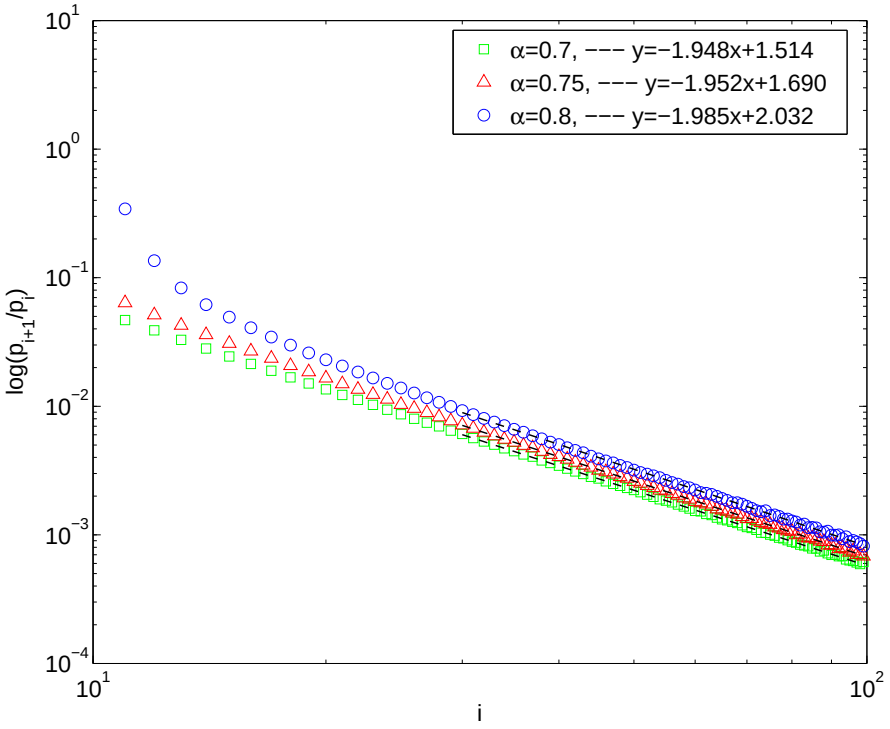

Figure S6: **Scaling Law and Convergence to p_c for the BFW model** (a) The position p_i of micro-transitions are well fitted by Eqn. S1 for $\alpha = 0.7, 0.75, 0.8$. Note that we display a log-log plot suggesting $\log \frac{p_{i+1}}{p_i} = Ai^{-b}$.

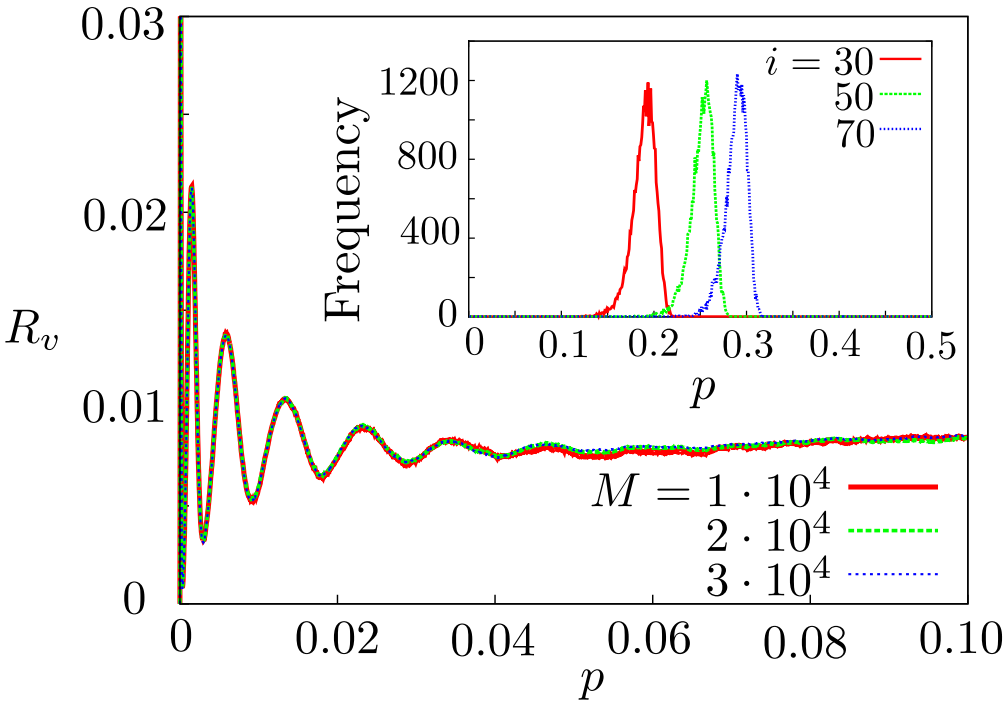

Figure S7: **Resonances and blurring in $\mathcal{R}_v$ for continuous percolation.** The relative variance of the order parameter for the ER model of size $N = 2^{25}$ obtained over three different numbers of realizations $M = 10^4$; $2 \cdot 10^4$; $3 \cdot 10^4$. The first peak in the plot marks the transition $C_1 : 3 \to 4$, the second $C_1 : 4 \to 5$ and so on. No peaks are seen for jumps for large i, due to overlapping broad distributions of the p_i, as illustrated in the inset for $i = 30, 50, 70$.

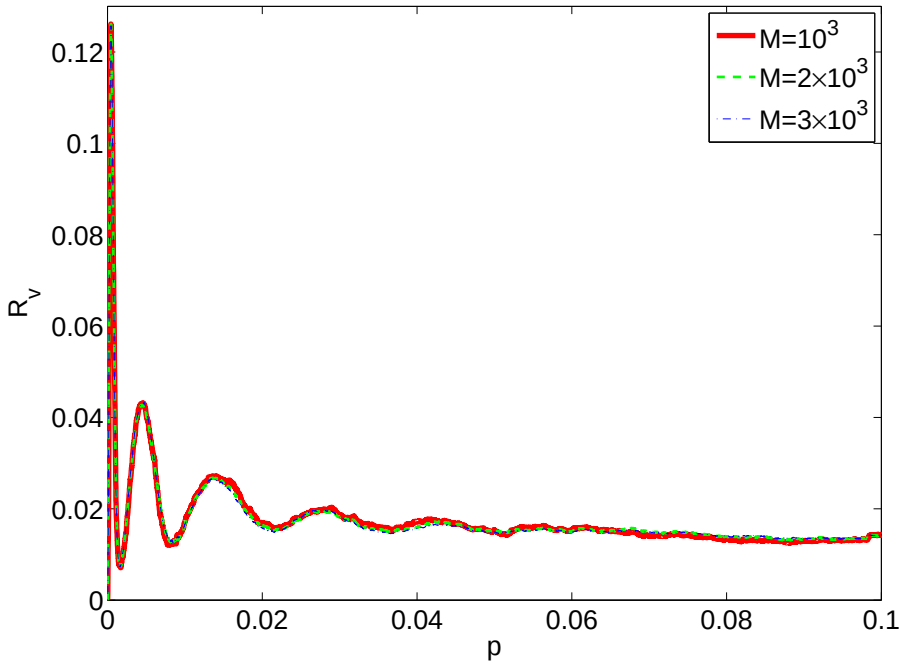

Figure S8: The relative variance of order parameter for 2D lattice percolation of size $N = 10^3 \times 10^3$ obtained over three different number of realizations $M = 10^3, 2 \times 10^3, 3 \times 10^3$. Remarkably, it shows a qualitatively similar behavior as for ER.